

# Efficient chaperone-mediated tubulin biogenesis is essential for cell division and cell migration in *C. elegans*

Victor F. Lundin<sup>a</sup>, Martin Srayko<sup>b,1</sup>, Anthony A. Hyman<sup>b</sup>, Michel R. Leroux<sup>a,\*</sup>

<sup>a</sup> Department of Molecular Biology and Biochemistry, Simon Fraser University, Burnaby, Canada

<sup>b</sup> Max-Planck-Institute of Molecular Cell Biology and Genetics, Dresden, Germany

Received for publication 8 May 2007; revised 17 October 2007; accepted 18 October 2007

Available online 24 October 2007

## Abstract

The efficient folding of actin and tubulin *in vitro* and in *Saccharomyces cerevisiae* is known to require the molecular chaperones prefoldin and CCT, yet little is known about the functions of these chaperones in multicellular organisms. Whereas none of the six prefoldin genes are essential in yeast, where prefoldin-independent folding of actin and tubulin is sufficient for viability, we demonstrate that reducing prefoldin function by RNAi in *Caenorhabditis elegans* causes defects in cell division that result in embryonic lethality. Our analyses suggest that these defects result mainly from a decrease in  $\alpha$ -tubulin levels and a subsequent reduction in the microtubule growth rate. Prefoldin subunit 1 (*pf1-1*) mutant animals with maternally contributed PFD-1 develop to the L4 larval stage with gonadogenesis defects that include aberrant distal tip cell migration. Importantly, RNAi knockdown of prefoldin, CCT or tubulin in developing animals phenocopy the *pf1-1* cell migration phenotype. Furthermore, reducing CCT function causes more severe phenotypes (compared with prefoldin knockdown) in the embryo and developing gonad, consistent with a broader role for CCT in protein folding. Overall, our results suggest that efficient chaperone-mediated tubulin biogenesis is essential in *C. elegans*, owing to the critical role of the microtubule cytoskeleton in metazoan development.

© 2007 Elsevier Inc. All rights reserved.

**Keywords:** Molecular chaperone; Prefoldin; CCT; Protein biogenesis; Actin; Tubulin; Tubulin homeostasis; Microtubule dynamics; Embryonic cell division; Distal tip cell migration

## Introduction

The eukaryotic cytoskeleton consists of an intricate network of dynamic protein filaments that are required for structural integrity, intracellular trafficking and cell motility. As the building blocks of microfilaments and microtubules, actin and tubulin make up a large portion of the total protein in most cells. Due to their high concentration, propensity to self-associate, and inability to fold unaided, newly-synthesized actin and tubulin represent a significant challenge to the protein biogenesis machinery of the cell (Hartl and Hayer-Hartl, 2002). In fact, actin and tubulin appear to have co-evolved with at least two molecular chaperones specifically required for

their biogenesis, namely prefoldin (PFD or GimC) and the chaperonin containing TCP-1 (CCT; also named TCP-1 Ring Complex or TRiC) (Willison, 1999; Leroux and Hartl, 2000).

The eukaryotic chaperonin CCT is an ATP-dependent protein folding machine assembled from two stacked rings of eight closely related subunits; these rings form a cylindrical cavity that encloses and assists the folding of nascent proteins (Llorca et al., 2000; Spiess et al., 2004). Prefoldin consists of six related proteins – two  $\alpha$ -type subunits and four  $\beta$ -type subunits, each with a long coiled-coil domain – that assemble to form a jellyfish-shaped oligomer (Siegert et al., 2000). The prefoldin hexamer binds non-native actin and tubulin with the tips of its tentacles and forms a transient ternary complex with CCT, delivering substrates into the cavity opening (Vainberg et al., 1998; Siegert et al., 2000; Martin-Benito et al., 2002; Zako et al., 2005).

A significant proportion of newly synthesized proteins reach their native states through interactions with CCT, although actin

\* Corresponding author.

E-mail address: [leroux@sfu.ca](mailto:leroux@sfu.ca) (M.R. Leroux).

<sup>1</sup> Current address: Department of Biological Sciences, University of Alberta, Edmonton, Canada.

and tubulin are among the most important substrates (Sternlicht et al., 1993; Thulasiraman et al., 1999). CCT function appears to be closely linked to multiple cellular processes including cell growth and proliferation (Yokota et al., 1999; Grantham et al., 2006), and all eight CCT genes are essential for viability in *Saccharomyces cerevisiae*. The notion that CCT plays a complex and fundamental role *in vivo* is underscored by the ongoing discovery of new substrates of CCT such as Cdc20 and polo-like kinase 1, which are regulators of the cell cycle (Camasses et al., 2003; Liu et al., 2005). The current paradigm for the regulation of CCT is that it cooperates with different chaperones in the folding of specific subsets of client proteins. In *S. cerevisiae*, for example, the folding of the WD40 protein Cdc55p involves the cooperation of Hsp70 with CCT, whereas CCT-mediated folding of actin and tubulin involves prefoldin activity that cannot be replaced by Hsp70 (Siegers et al., 2003). Recent work has characterized the role of the novel CCT cofactor phosphuducin-like protein 3, which negatively regulates CCT-mediated actin and tubulin folding by slowing the rate of ATP-hydrolysis; interestingly, its activity appears to antagonize the action of prefoldin (McLaughlin et al., 2002; Stirling et al., 2006). Additional work on the role of cofactors regulating CCT function has characterized phosphuducin-like protein 2 as being essential in *S. cerevisiae* for cytoskeletal protein function (Stirling et al., 2007).

Detailed *in vitro* studies have revealed that prefoldin binds to nascent polypeptides at the ribosome and maintains them in a folding-competent state until it can deliver them to CCT for folding in a protected compartment (Vainberg et al., 1998; Hansen et al., 1999; Leroux et al., 1999; Siegers et al., 1999). The molecular mechanism of prefoldin substrate binding and the docking of the prefoldin hexamer with the chaperonin have been well characterized (Sieger et al., 2000; Martin-Benito et al., 2002; Lundin et al., 2004; Okochi et al., 2004; Simons et al., 2004; Zako et al., 2005; Martin-Benito et al., 2007). Pulse-chase and co-immunoprecipitation experiments in yeast cells have shown that prefoldin deletions cause a slowed release of folded actin from CCT, and an increase in the amount of non-native actin released into the cytosol (Siegers et al., 1999). These results suggest that prefoldin stimulates CCT substrate release and/or that prefoldin binds partially folded intermediates released from CCT and returns them for further rounds of folding (Vainberg et al., 1998; Siegers et al., 1999). In either case, it is clear that prefoldin increases the overall yield of CCT-mediated cytoskeletal protein folding, since the steady-state levels of actin,  $\alpha$ - and  $\beta$ -tubulin polypeptides are reduced in prefoldin-depleted yeast cells (Geissler et al., 1998; Lacefield and Solomon, 2003; Lacefield et al., 2006).

There is no conclusive evidence for *bona fide* substrates of the prefoldin-dependent CCT-mediated folding pathway other than actin and tubulin, although additional proteins (VHL, *c-myc* and MSH4) have been shown to bind individual subunits of prefoldin (Tsuchiya et al., 1996; Mori et al., 1998; Her et al., 2003). Several pieces of evidence also point to  $\gamma$ -tubulin as a putative prefoldin substrate. Prefoldin knockout mutations suppress the toxic effects of overexpressed  $\gamma$ -tubulin, enhance  $\gamma$ -tubulin mutant phenotypes, and prefoldin co-immunopreci-

pitates with overexpressed  $\gamma$ -tubulin; however, the physiological relevance of this relationship has not been determined (Geissler et al., 1998).

In *S. cerevisiae*, deletion of one or more prefoldin genes causes microfilament and microtubule defects that ultimately lead to a slow growth phenotype (Vainberg et al., 1998; Geissler et al., 1998; Siegers et al., 1999). A triple deletion of 3 prefoldin genes has the same quantitative effect on the rate of actin folding as a single prefoldin deletion and cells with all six prefoldin genes deleted are still viable (Siegers et al., 1999, 2003). Prefoldin deletion strains fold actin at approximately 20% of the wild-type rate, but are able to accumulate approximately 50% of the wild-type concentration of actin (Siegers et al., 1999). Thus, although prefoldin acts non-redundantly with respect to CCT, yeast prefoldin mutants are viable because they can accumulate reduced but sufficient concentrations of actin and tubulin via slow, prefoldin-independent folding pathways.

In contrast to actin or  $\gamma$ -tubulin,  $\alpha$ - and  $\beta$ -tubulin require several additional stages of stabilization and assembly after the release from CCT (Gao et al., 1992; Melki et al., 1993). The tubulin folding cofactors A, B, C, D and E have evolved specific roles regulating the assembly of the  $\alpha/\beta$ -tubulin heterodimer from quasi-native  $\alpha$ - and  $\beta$ -tubulin monomers (Lopez-Fanaraga et al., 2001). In addition, tubulin synthesis is subject to an autoregulatory mechanism whereby the concentration of tubulin feeds back on the stability of ribosome-bound tubulin mRNA through co-translational recognition of the amino terminal tetrapeptide MREI (Gay et al., 1989; Savage et al., 1994; Ellis et al., 2003). Recent evidence suggests that tubulin is also regulated by ubiquitin-proteasome-mediated degradation. In particular, cofactor E-like, a protein identified based on its similarity to the tubulin folding cofactor E, has been implicated in  $\alpha$ -tubulin degradation, suggesting that biogenesis and degradation of  $\alpha$ -tubulin may be closely linked (Bartolini et al., 2005).

Although significant data has been collected regarding the functions of prefoldin and CCT at the molecular level, the cellular and developmental processes that depend on these chaperones in metazoans has not been characterized. In *Caenorhabditis elegans*, several large-scale RNA-mediated interference (RNAi) screens have identified subunits of prefoldin, CCT and the tubulin folding cofactors D and E as being required for embryonic viability (Fire et al., 1998; Fraser et al., 2000; Maeda et al., 2001; Simmer et al., 2003; Kamath et al., 2003). Studies of RNAi-treated embryos using time-lapse microscopy have implicated prefoldin, CCT and tubulin folding cofactor D in the early steps of *C. elegans* embryogenesis (Gönczy et al., 2000; Zipperlen et al., 2001; Sönnichsen et al., 2005). More targeted approaches have identified members of the prefoldin and CCT gene families, as well as the homologs of phosphuducin-like protein 3 and the tubulin folding cofactor D, as being associated with the proper function of the microtubule cytoskeleton in the early *C. elegans* embryo (Le Bot et al., 2003; Ogawa et al., 2004; Srayko et al., 2005).

In the present study, we conduct a comprehensive analysis of the essential roles of prefoldin and CCT in *C. elegans*. We

present the expression patterns of transgenic prefoldin and CCT subunits in the multicellular organism as well as the embryonic and germline expression of endogenous prefoldin subunit 6 (*pfid-6*). We examine the steady-state concentration of putative prefoldin substrates in prefoldin-deficient embryos and show that the intracellular  $\alpha$ -tubulin concentration is strongly reduced compared to the concentrations of actin and  $\gamma$ -tubulin. We show that prefoldin depletion results in a decrease in the microtubule growth rate and that the cellular phenotypes closely resemble those of tubulin deficiency, suggesting that the predominant role for prefoldin in the embryo may be to ensure efficient folding of nascent tubulin polypeptides. We also demonstrate a distal tip cell migration defect in the developing gonads of homozygous *pfid-1* mutant animals, which is also present in animals with low-level RNAi knockdown of prefoldin, CCT or tubulin. Our results suggest that efficient chaperone-mediated tubulin biogenesis is essential in *C. elegans* for the renewal of the functional tubulin pool during embryonic cell division and distal tip cell migration.

## Materials and methods

### *C. elegans* culture and strains

Worms were maintained using standard techniques (Brenner, 1974). Strains: N2 (wild-type); BC10082 ( $P_{pfid-5}$ :GFP); BC10433 ( $P_{cct-2}$ :GFP); BC12510 ( $P_{cct-7}$ :GFP); AZ244; OD3; TH33; JJ1473; TH66; VC1013 (*pfid-1(gk526)*) and VC1032 (*pfid-4(gk430)*). VC1013 and VC1032 were obtained from the *C. elegans* Reverse Genetics Core Facility (University of British Columbia, Vancouver, BC, Canada), analyzed for gene duplications and backcrossed 3 times. To generate transcriptional fusions of *pfid-1* and *pfid-6*, putative regulatory sequences 647 bp upstream of *pfid-1* and 678 bp upstream of *pfid-6* were fused to the GFP coding sequence as described (Ansley et al., 2003). For translational fusions of *pfid-1* and *pfid-3*, putative regulatory sequences 647 bp upstream of *pfid-1* and 2121 bp upstream of *pfid-3*, plus the coding and all intronic sequence for each gene, were used. Integrated arrays were obtained by X-ray irradiation (McKay et al., 2003) and backcrossed 3 times.

### Antibody production

PFD-6 cDNA was obtained from Dr. Yuji Kohara. *pfid-6* cDNA was subcloned into pRSET6a and expressed in BL21 DE3 *Escherichia coli* cells. PFD-6 protein was purified from the insoluble fraction by Q-Sepharose anion-exchange chromatography under denaturing conditions (8 M urea). Pure, denatured PFD-6 was injected into a rabbit at 1 mg/ml in MPL+TDM+CWS adjuvant (Sigma, cat#M-6661) at 3-week intervals until a band was detectable in *C. elegans* embryo lysate by western blot. Crude rabbit PFD-6 antiserum was affinity-purified against membrane-bound recombinant PFD-6 protein.

### Western blotting

Alkaline/hypochlorite-isolated embryo lysates were normalized for total protein and separated by SDS-PAGE, transferred to nitrocellulose membrane and stained with Ponceau S to visualize total protein. Membranes were probed with 1:200 affinity-purified rabbit polyclonal PFD-6 antiserum, 1:1000 monoclonal mouse GFP antibody (Roche, cat#1814460), 1:1000 monoclonal mouse  $\alpha$ -tubulin antibody (Sigma, cat#T9026), 1:2000 monoclonal mouse actin antibody (Chemicon, cat#MAB1501), or 1:500 monoclonal mouse  $\gamma$ -tubulin antibody (Sigma, cat#T6557) and 1:50,000 HRP-conjugated goat anti-rabbit (Sigma, cat#A-0545) or goat anti-mouse (Sigma, cat#A-0168) secondary antibodies. Bands were visualized using ECL Plus (GE Healthcare, cat#RPN2132) and a Typhoon Phosphorimager system (Molecular Dynamics). Quantitation was done using ImageQuant software (Molecular Dynamics).

### RNAi

For RNAi by feeding, cDNAs for the six prefoldin genes were obtained from Dr. Yuji Kohara and subcloned into the *NotI* sites of the pL4440 vector (Timmons and Fire, 1998), transformed into HT115 *E. coli* and seeded onto NGM plates supplemented with 100  $\mu$ g/ml ampicillin, 10  $\mu$ g/ml tetracycline and 1 mM IPTG. For *cct-1* and *tba-2*, available RNAi constructs were used (Kamath et al., 2003). For RNAi by injection, ssRNA was synthesized from PCR product or linearized pL4440 vector templates using the RiboMax kit (Promega), annealed and injected at  $\sim$ 1 mg/ml into both gonad arms of young adult animals.

### Immunofluorescence

Gonads were dissected from adult wild-type worms and fixed in 3% formaldehyde, 0.25% glutaraldehyde, 100 mM  $K_2HPO_4$  (pH 7.2) for 2 h with a 100% methanol post-fix. Embryos were pre-fixed in 3% formaldehyde, 0.25% glutaraldehyde, 100 mM  $K_2HPO_4$  (pH 7.2), frozen in liquid nitrogen, thawed and fixed for 15 min at room temperature. Fixed embryos and gonads were stained with 1:20 affinity-purified rabbit PFD-6 antiserum and 1:1000 AlexaFluor 488-conjugated (Molecular Probes) goat anti-rabbit secondary antibody, or secondary antibody alone, with DAPI included in the penultimate wash.

### Microscopy

Early embryos were dissected from control or RNAi-treated hermaphrodites (approximately 3 h before the onset of 100% lethality in laid eggs) (Supplementary Table 1) and mounted on 2% agarose pads. Embryos were observed through a 100 $\times$  Plan NEOFLUAR objective (NA 1.3) mounted on a Zeiss Axioskop microscope. Images were captured and analyzed using a Hamamatsu Orca-ER or a QImaging Retiga-EXi camera and Northern Eclipse (Empix Imaging) software or Openlab (Improvision) software. To record the first two cell divisions, DIC and GFP images were captured every minute for a maximum of 15 min. Control embryos hatched under the coverslip after microscopy. Worms were anesthetized with 25 mM levamisole and mounted on 2% agarose pads.

### Image analysis

Cortical cytoplasmic streaming was estimated by manually tracking the movement of yolk granules as described (Hird and White, 1993; O'Connell et al., 2000). Fluorescence intensities of GFP: TBA-2, GFP: TBB-2, GFP: TBG-1 and GFP: HIS-11 in *pfid-3(RNAi)* and *control(RNAi)* embryos were quantified using Northern Eclipse software. For each GFP-tagged protein, the total pixel intensity of the relevant fluorescent signal in a constant area was quantified at several points of the cell cycle, averaged over the cell cycle and reported as a fraction of fluorescence in control embryos ( $n=10$  embryos). Microtubule growth rates were measured by recording the behaviour of microtubule + ends decorated with GFP-tagged EB2 in TH66 worms injected with the indicated dsRNA (Fig. 2D) as described (Srayko et al., 2005).

## Results

### *Prefoldin and CCT expression patterns overlap in multiple tissues*

If prefoldin and CCT are required in the same pathway for cytoskeletal protein folding, subunits of each complex would be expected to exhibit similar expression patterns. We therefore compared the spatial and temporal expression patterns of GFP reporter constructs driven by the promoter sequences (see Materials and methods) of three prefoldin genes, *pfid-1*, *pfid-5* and *pfid-6*, and two CCT genes, *cct-2* (CCT $\beta$ ) and *cct-7*

(CCT $\eta$ ). Although the intensity of the fluorescence was variable, the expression patterns of these transgenes were similar and could be observed in various tissues throughout the animal, consistent with a ubiquitous expression of prefoldin and CCT subunits (Supplementary Fig. 1A). GFP expression was consistently observed in the muscles of the head, pharynx, body-wall and vulva of adult worms (Supplementary Fig. 1A). We also examined the localization of GFP-tagged PFD-1 and PFD-3 proteins (see Materials and methods). As well as being expressed in the same cell types as the promoter–GFP reporter constructs, PFD-1::GFP and PFD-3::GFP expressed from integrated transgenic arrays were present in the cytoplasm of many additional cells throughout the animal (Supplementary Figs. 1B, C). This expression pattern is similar to the homolog of phosphocin-like protein 3, which has been shown to function together with prefoldin to regulate CCT-mediated protein folding in yeast (Ogawa et al., 2004; Stirling et al., 2006). While it is possible that some unknown endogenous regulatory elements were omitted in these GFP reporter constructs, our data suggests that prefoldin and CCT are likely ubiquitously expressed.

Based on the requirement for protein synthesis (and therefore folding) in actively proliferating cells, we expected that prefoldin and CCT expression would be detectable in the early embryo and the adult germline. However, we did not

observe any expression of our transgenic reporter genes in these tissues (Supplementary Fig. 1), likely as a result of germline silencing of the transgenes (Kelly et al., 1997). In order to assess the expression in the germline and the embryo, a rabbit polyclonal antiserum was raised against full-length recombinant PFD-6 protein (see Materials and methods). The affinity-purified rabbit PFD-6 antiserum recognizes a single band in a western blot analysis of wild-type embryo lysate (Fig. 1A). Consistent with a cytosolic distribution for prefoldin, immunocytochemistry with the PFD-6 antibody on control embryos revealed a diffuse non-nuclear staining in all cells (Fig. 1B). Both the immunofluorescence signal and the protein detection by western blot were significantly reduced in *pfid-6(RNAi)* embryos, confirming the specificity of the antibody (Figs. 1A,B). We also observed diffuse cytoplasmic staining in dissected gonads (Fig. 1C). Since available CCT-1 antisera were not suitable for immunostaining (Leroux and Candido, 1997), we could not confirm the presence of CCT in the germline and embryo; however, CCT transcripts can be detected in most tissues and developmental stages of the worm including gonads, oocytes and embryos (Hill et al., 2000; McKay et al., 2003; Chen et al., 2005). Taken together, the expression data for the subunits of prefoldin and CCT are consistent with a ubiquitous role in cytosolic protein folding of the metazoan *C. elegans*.

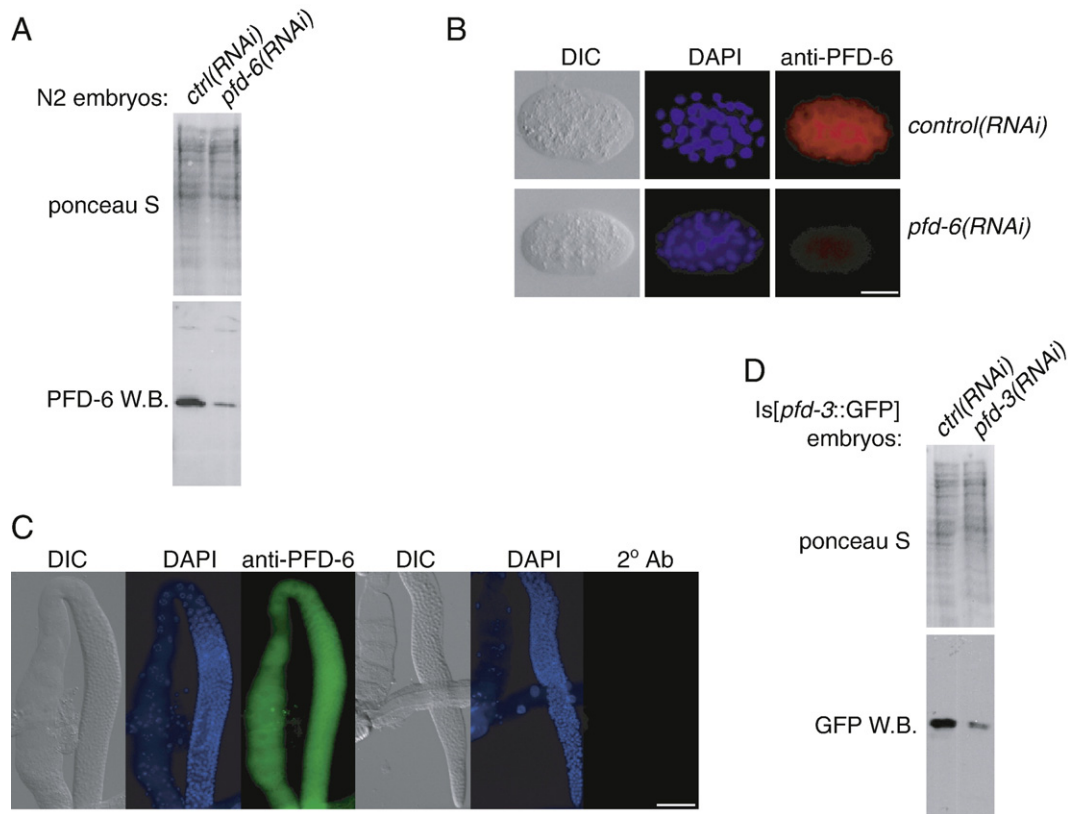


Fig. 1. Prefoldin is expressed in embryos and gonads and the RNAi protocol efficiently removes target protein. (A) Western blot analyses of *control(RNAi)* and *pfid-6(RNAi)* embryo lysates using PFD-6 antibody showing effective target gene knockdown. (B) Non-nuclear anti-PFD-6 staining was observed in embryonic blastomeres which was strongly reduced in *pfid-6(RNAi)* embryos. Scale bar=20  $\mu$ m. (C) Endogenous PFD-6 is expressed throughout the adult gonad. Scale bar=50  $\mu$ m. (D) anti-GFP western blot analysis of *control(RNAi)* and *pfid-3(RNAi)* embryo lysates from worms expressing transgenic *pfid-3::GFP*; see Materials and methods.

### *Prefoldin and CCT are required for embryogenesis*

Data from yeast (Siegers et al., 1999, 2003) and mammalian cells (Grantham et al., 2006) have shown that the functions of the prefoldin and CCT chaperone complexes are eliminated by removal of individual subunits. Previous studies in *C. elegans* have shown that RNAi knockdown of individual prefoldin or CCT subunits caused a variably penetrant embryonic lethal phenotype (Fraser et al., 2000; Maeda et al., 2001; Kamath et al., 2003; Simmer et al., 2003; Sönnichsen et al., 2005). To examine the roles of prefoldin and CCT in *C. elegans* in greater detail, we conducted a time-course of embryonic lethality as a result of RNAi targeting individual genes of each chaperone family. We found that RNAi knockdown of individual prefoldin or CCT subunit genes resulted in fully penetrant embryonic lethality, with the notable exception of the PFD-4 subunit, which had no discernable phenotype (Supplementary Table 1). RNAi knockdown of *cct-1* resulted in a more severe phenotype than RNAi knockdown of the prefoldin genes since it caused a maternal sterile phenotype in addition to embryonic lethality. Although the time of onset of the embryonic lethal phenotype varies, interfering with the function of prefoldin or CCT clearly has a similar and profound effect on embryonic viability.

To test the target gene knockdown efficiency of our RNAi procedure, we analyzed embryo lysates from RNAi-treated worms by western blot. Using the PFD-6 antibody, we observed a strong knockdown of endogenous PFD-6 protein in *pfid-6* (RNAi) embryos (Fig. 1A). We also observed strong knockdown of transgenically expressed PFD-3::GFP protein in *pfid-3* (RNAi) embryos using an antibody to GFP (Fig. 1D). The knockdown of endogenous PFD-3 protein caused by *pfid-3* (RNAi) in wild-type worms is likely higher than that observed for transgenically expressed PFD-3::GFP, and likely represents a near-maximal RNAi knockdown of prefoldin function.

The fact that *pfid-4*(RNAi) produced no phenotype was surprising given that both yeast and human PFD-4 orthologs are integral to the function of the prefoldin chaperone complex (Siegers et al., 1999; Simons et al., 2004). In order to test if the lack of an observable phenotype was due to a lack of RNAi penetrance, we obtained a mutant strain from the *C. elegans* Knockout Consortium in which the entire coding region of *pfid-4* is removed (Supplementary Fig. 2). Consistent with the lack of a *pfid-4*(RNAi) phenotype, worms homozygous for the *pfid-4* (*gk430*) allele have no visible morphological or developmental phenotypes (Supplementary Fig. 2). We then performed a phylogenetic analysis of the  $\beta$ -type prefoldin genes (i.e. *pfid-1*, *pfid-2*, *pfid-4* and *pfid-6*) from several eukaryotic organisms and found that *C. elegans* and *C. briggsae* PFD-4 have diverged from their animal orthologs compared to the other  $\beta$ -type prefoldin genes (Supplementary Fig. 2). Taken together, these results suggest that PFD-4 may have been recruited for a different (non-chaperone) function in the nematode. This is especially interesting since several  $\beta$ -type prefoldin subunits, including PFD-2, PFD-6 and a PFD-4-related protein that is absent from the *C. elegans* genome, also participate in a complex with the unconventional prefoldin RPB5 interactor

(URI) that mediates a transcriptional response downstream of TOR kinase (Gstaiger et al., 2003).

### *Prefoldin is required for maintaining proper tubulin homeostasis and microtubule dynamics*

Evidence from yeast suggests that a decrease in prefoldin function causes a greater proportion of newly synthesized substrate polypeptides to be released from CCT into the cytosol in an improperly folded state (Siegers et al., 1999). Such protein species would be prone to aggregation, and we predicted that they would either form inclusions or be removed by regulated proteolysis in the *C. elegans* embryo. To test this, we compared the steady-state levels of putative prefoldin substrates in whole-cell lysates from *control*(RNAi) and *pfid-3*(RNAi) embryos by western blot analysis (Fig. 2A). We found that when prefoldin function was inhibited, the concentration of  $\alpha$ -tubulin in the embryo was decreased by at least 95% (Fig. 2B). In addition, we did not detect any immunogenic detergent-insoluble  $\alpha$ -tubulin aggregates that were left in the stacking gel during electrophoresis (data not shown). In contrast, there was only a 30% decrease in the total concentration of actin polypeptides and no significant decrease in the amount of  $\gamma$ -tubulin (Fig. 2B). We did not detect any immunogenic detergent-insoluble actin or  $\gamma$ -tubulin in the stacking gel (data not shown). It is possible that prefoldin depletion causes a greater increase in the proportion of misfolded actin or  $\gamma$ -tubulin that is not degraded and does not form detergent-insoluble aggregates, which we did not test for. However, given our phenotypic analyses (see below), we favour the interpretation that actin and  $\gamma$ -tubulin are not drastically affected in the *C. elegans* embryo (see Discussion).

In a previous study, *C. elegans* CCT and phosphocysteine-like protein 3 were shown to be required for fast microtubule growth in the early embryo, whereas *pfid-1* was reported to have an effect on microtubule nucleation, but not the microtubule polymerization rate (Srayko et al., 2005). In light of our current observations of strongly reduced  $\alpha$ -tubulin levels, we decided to conduct a thorough test on the effect of prefoldin depletion on microtubule polymerization under the conditions used in this study. We used a *C. elegans* strain expressing GFP-tagged EBP-2 (end-binding protein 2, a homolog of EB1), which decorates the tips of individual microtubules, to determine the growth rate of microtubules *in vivo* (Srayko et al., 2005). In embryos from these worms, EBP-2::GFP fluorescent particles can be observed at the centrosomes, where extensive microtubule nucleation takes place, and also as discrete spots moving away from the spindle poles (Fig. 2C, Movie S1). This dynamic pattern was present to a reduced extent in *pfid-3*(RNAi) embryos, consistent with the presence of fewer and/or shorter microtubules (Fig. 2C, Movie S2). Using pattern-recognition software to track the movement of individual EBP-2::GFP spots over time, we found that decreasing the function of each prefoldin subunit by RNAi (except for the redundant *pfid-4*) caused a significant reduction of the microtubule growth rate from 0.7  $\mu\text{m/s}$  to approximately 0.4  $\mu\text{m/s}$  (Fig. 2D). Since microtubule polymerization is proportional to the concentration of free  $\alpha/\beta$ -tubulin heterodimers (Mitchison and Kirschner, 1984; Walker et al., 1988),

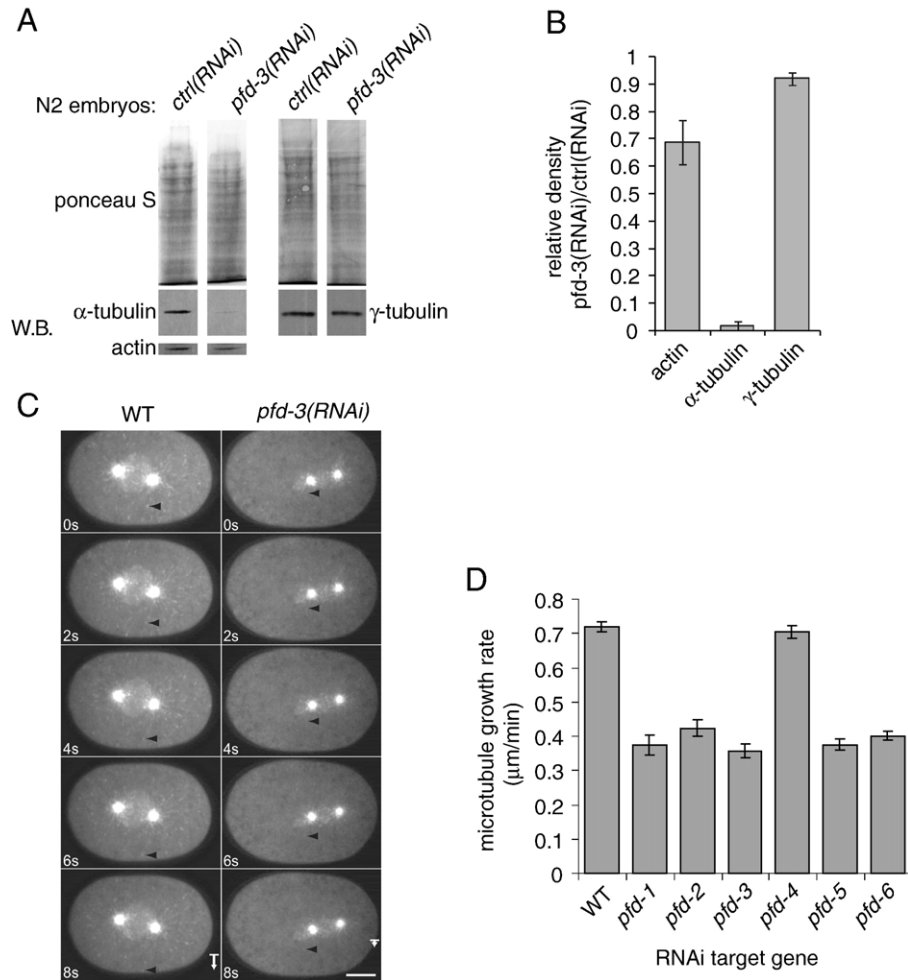


Fig. 2. Prefoldin is required for maintaining proper  $\alpha$ -tubulin levels and microtubule dynamics. (A) Anti- $\alpha$ -tubulin, anti-actin and anti- $\gamma$ -tubulin western blot and Ponceau S staining of *control(RNAi)* and *pfd-3(RNAi)* embryo lysates normalized for total protein. (B) Quantitation of steady-state levels of putative prefoldin substrates; see Materials and methods. (C) Image series showing movement of *ebp-2::GFP* spots at 2-s intervals in wild-type and *pfd-3(RNAi)* embryos. Black arrowheads indicate the position of the same particle in each image. White arrows indicate distance of travel for the given particles over an 8-s interval. Scale bar = 10  $\mu\text{m}$ . (D) Microtubule growth rates in embryos depleted for the indicated prefoldin subunits by RNAi; see Srayko et al., 2005.

these results strongly suggest that prefoldin depletion causes a reduced efficiency of tubulin folding, leading to a reduced level of  $\alpha$ -tubulin and a decrease in the concentration of assembly-competent  $\alpha/\beta$ -tubulin heterodimers being generated.

#### *Microfilament function is not severely compromised in prefoldin-deficient embryos*

Based on previous reports linking prefoldin to actin biogenesis (Vainberg et al., 1998; Siegers et al., 1999; Stirling et al., 2006), and our observation that actin levels were not strongly reduced in the absence of wild-type levels of prefoldin (Fig. 2B), we examined the function of the microfilament cytoskeleton in prefoldin-deficient embryos (Fig. 3). Filamentous  $\beta$ -actin is present throughout the cortex of the *C. elegans* embryo and is required, along with the non-muscle myosin NMY-2, for the actomyosin contractile activity associated with pseudocleavage, cytoplasmic flow and cytokinesis (Strome and Wood, 1983; Guo and Kemphues, 1996). We used time-lapse micro-

scopy of live embryos expressing GFP-tagged NMY-2 as a way to assess the integrity/function of the cortical microfilament cytoskeleton (Munro et al., 2004). In wild-type embryos, NMY-2::GFP/actin patches localize to the anterior cortex during pseudocleavage, then become uniformly distributed around the cell periphery during mitosis and NMY-2::GFP finally accumulates at the cytokinetic cleavage furrow (Fig. 3A).

RNAi-knockdown of *pfd-3* did not have a discernable effect on the localization of NMY-2::GFP/actin patches. In *pfd-3(RNAi)* embryos, NMY-2::GFP was anteriorly polarized in patches during pseudocleavage and localized to contractile regions in the membrane, including the cytokinetic cleavage furrows (10/10 embryos) (Fig. 3B). Our time-lapse recordings of *pfd-3(RNAi)* embryos also revealed that significant contractile activity was present at the cell cortex and although the timing and the specification of the cleavage plane was often disrupted, both pseudocleavage and cytokinesis still occurred (see below) (Figs. 3 and 5, Table 1). Even the most severely affected *pfd-3(RNAi)* embryos (i.e. at >32 h of the RNAi time-

course) that failed to complete cytokinesis during the first cell cycle, eventually succeeded in cell cleavage, yielding a terminal phenotype with many cytoplasts (data not shown). These results show that cortical actomyosin activity is at least partially intact in *pfd-3(RNAi)* embryos, and taken together with the observation that the total concentration of actin is not dramatically reduced, suggest that newly synthesized actin may not represent a significant substrate load for prefoldin in the early embryo.

#### *Prefoldin is essential for microtubule function in the early embryo*

To directly test the effect of prefoldin disruption on the microtubule cytoskeleton, we compared the overall structure of the mitotic spindle in *pfd-3(RNAi)* and *control(RNAi)* embryos expressing GFP-tagged  $\alpha$ -tubulin (GFP::TBA-2) and  $\beta$ -tubulin (GFP::TBB-2) using time-lapse DIC and fluorescence microscopy (Fig. 4). In addition to pronuclear rotation and spindle position defects that are visible by DIC (see Fig. 5), we noticed several specific aspects of microtubule malfunction in *pfd-3(RNAi)* embryos. The mitotic spindles were small, with closely spaced spindle poles in prometaphase and metaphase (data not shown). During anaphase, there was a reduction in the density of interpolar spindle microtubules and the spindle structure was lacking in symmetry (Fig. 4B). In some *pfd-3(RNAi)* embryos, the spindle architecture was disrupted due to improper positioning of the centrosomes relative to the male and female pronuclei prior to spindle assembly (Fig. 4B).

Although our live imaging procedure did not allow us to visualize individual microtubules, we noticed a lower intensity of GFP::TBA-2 and GFP::TBB-2 fluorescence radiating from the spindle poles in prefoldin-deficient embryos, suggesting a reduction in the number or length of microtubules (Fig. 4B).

When we compared the total fluorescence intensity of GFP-tagged marker proteins in *pfd-3(RNAi)* and control embryos, we found that the GFP::TBA-2 and GFP::TBB-2 signals were reduced by 65% and 50%, respectively, whereas the fluorescence of a GFP-tagged control protein, GFP::HIS-11, was unchanged (Fig. 4C). This suggests that knockdown of prefoldin function causes a reduction in the levels of fluorescent GFP-tagged  $\alpha$ - and  $\beta$ -tubulin, which is consistent with the observed reduction in the amount of endogenous  $\alpha$ -tubulin (Figs. 2A, B) and with a subsequent reduction in the overall number and/or length of microtubules.

#### *Centrosome function is not severely altered in prefoldin-deficient embryos*

An interaction between prefoldin and  $\gamma$ -tubulin has been reported previously and suggests that CCT-mediated  $\gamma$ -tubulin folding may also involve prefoldin function (Melki et al., 1993; Geissler et al., 1998). In addition, some of the microtubule defects we observe in prefoldin-deficient embryos could be caused by a primary deficiency in  $\gamma$ -tubulin-dependent microtubule nucleation (Hannak et al., 2002). We therefore examined the localization of GFP-tagged  $\gamma$ -tubulin in *pfd-3(RNAi)* embryos (Supplementary Fig. 3). In *C. elegans*, the sperm contributes a centriole pair to the oocyte upon fertilization. Since the paternal germline is relatively resistant to RNAi, we avoided possible paternal rescue by examining embryos in the second cell division, where *de novo* centriole duplication relies on maternally contributed components (Kirkham et al., 2003; Dammermann et al., 2004). In all (11/11) two-cell *pfd-3(RNAi)* embryos recorded, the posterior P1 cell contained two centrosomes that migrated to opposite sides of the P1 nucleus, indicating that centrosome duplication and migration were not

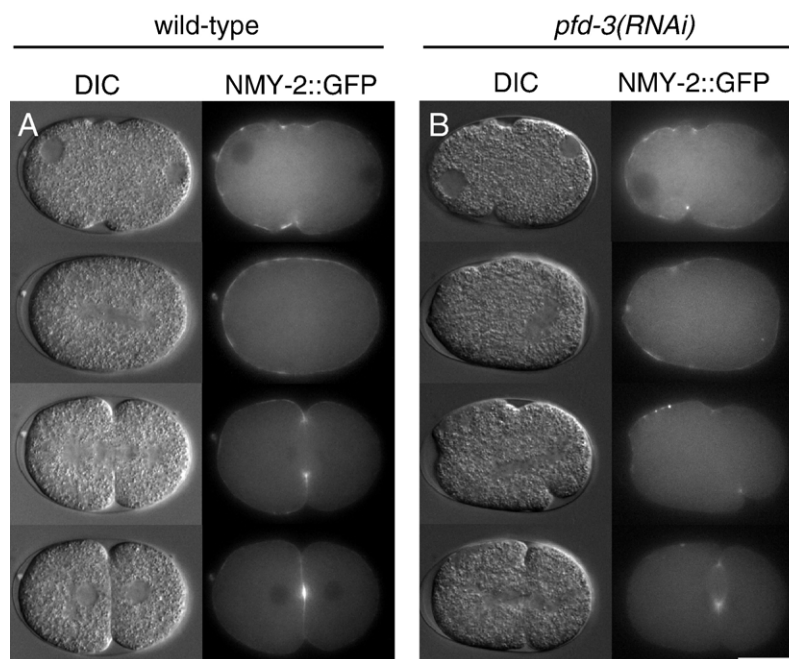
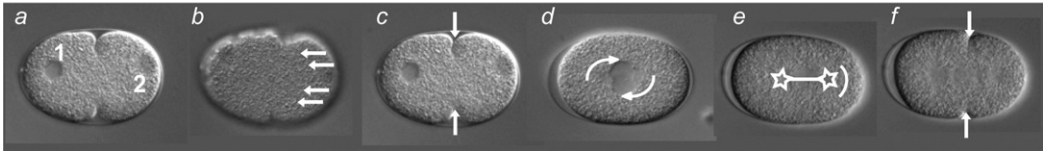


Fig. 3. Microfilament-dependent furrowing and NMY-2::GFP localization are not significantly affected in *pfd-3(RNAi)* embryos. Scale bar=20  $\mu$ m.

Table 1  
Summary of cell division phenotypes caused by RNAi knockdown of prefoldin, CCT or tubulin



RNAi target	RNAi method	Meiosis <sup>a</sup>	Cytoplasmic streaming <sup>b</sup> μm/min	Pseudo-cleavage furrow <sup>c</sup>	Pronuclear rotation <sup>d</sup>	Anaphase spindle position <sup>e</sup>	Cleavage furrow position <sup>f</sup>
(pL4440)	Feeding	100% (26)	6.3±0.3 (7)	100% (26)	100% (26)	100% (26)	100% (26)
<i>pf<sub>d</sub>-3</i>	Injection	78% (9)	2.2±0.8 (8)	100% (8)	0% (7)	10% (10)	20% (10)
<i>cct-1</i>	Injection	33% (9)	3.7±1.0 (8)	100% (4)	13% (8)	11% (9)	60% (5)
<i>tba-2</i> *	Feeding	83% (6)	1.9±1.1 (8)	100% (5)	17% (6)	17% (6)	20% (5)

Wild-type embryos shown with anterior to the left.

<sup>a</sup> % of embryos that contained only two pronuclei; ( $n$ =# of embryos).

<sup>b</sup> Horizontal anterior velocity of cortical cytoplasmic granules; mean±SEM; ( $n$ =# of granules; see Materials and methods).

<sup>c</sup> % of embryos that displayed a pseudo-cleavage furrow; ( $n$ =# of embryos).

<sup>d</sup> % of embryos that completed pronuclear rotation to align the centrosomes on the A–P axis; ( $n$ =# of embryos).

<sup>e</sup> % of embryos that had a stable horizontal spindle position during anaphase (except posterior rocking as in wild-type embryos).

<sup>f</sup> % of embryos that had two cytokinetic cleavage furrows ingressing perpendicular to the A–P axis; ( $n$ =# of embryos).

\* *tba-2(RNAi)* likely targets the nearly identical  $\alpha$ -tubulin TBA-1 as well (Wright and Hunter, 2003; Phillips et al., 2004).

affected, whereas spindle positioning defects were observed as in single-celled embryos (Supplementary Fig. 3). Furthermore, we did not detect a significant change of the GFP::TBG-1 fluorescence intensity in *pf<sub>d</sub>-3(RNAi)* embryos compared to *control(RNAi)* embryos (Fig. 4C). Taken together with the fact that we did not detect a significant change in the steady-state levels of  $\gamma$ -tubulin (Fig. 2A), these results suggest that the microtubule defects we observe in *pf<sub>d</sub>-3(RNAi)* embryos are not due primarily to a  $\gamma$ -tubulin deficiency, and that  $\gamma$ -tubulin may not be an important substrate for prefoldin in the early embryo.

#### Disruption of prefoldin or CCT function causes a variety of defects in cell division

To examine the downstream effects of decreased prefoldin and CCT function on *C. elegans* embryogenesis, we used time-lapse DIC and fluorescence microscopy to record the first cell division in embryos subjected to RNAi targeting either chaperone. We then assessed the correct execution of the following distinct events: pronuclear rotation, spindle positioning, cytokinetic cleavage furrow formation, meiosis, cytoplasmic streaming, pseudocleavage furrow formation and chromosome segregation (Table 1).

#### Rotation of the pronuclear-centrosome complex

One of the most prevalent phenotypes observed in both *pf<sub>d</sub>-3(RNAi)* and *cct-1(RNAi)* embryos was a lack of rotation of the pronuclear-centrosome complex. Specifically, 7/7 *pf<sub>d</sub>-3(RNAi)* embryos and 7/8 *cct-1(RNAi)* embryos failed to rotate (Table 1, Fig. 5). Disruption of microtubules by pharmacological treatment, RNAi-depletion of tubulin, or by a failure to downregulate expression of the microtubule-severing activity of MEI-1/MEI-2/katanin, all result in pronuclear rotation defects (Hyman and White, 1987; Quintin et al., 2003; Wright

and Hunter, 2003; Phillips et al., 2004). Interestingly, RNAi disruption of phosphatidylinositol-3-OH kinase-like protein 3, which in yeast is implicated in prefoldin/CCT-mediated folding, also causes defects in pronuclear rotation (Ogawa et al., 2004; Stirling et al., 2006).

#### Mitotic spindle positioning

The same treatments that abolish pronuclear rotation also cause spindle positioning defects (Hyman and White, 1987; Labbe et al., 2003; Wright and Hunter, 2003; Phillips et al., 2004). Consistent with these observations, we observe a correlation between pronuclear rotation and spindle position defects in *pf<sub>d</sub>-3(RNAi)* and *cct-1(RNAi)* embryos (Table 1). Nearly all *pf<sub>d</sub>-3(RNAi)* embryos (9/10) and *cct-1(RNAi)* embryos (8/9) displayed aberrant positioning of the mitotic spindle (Table 1, Fig. 5).

#### Cytokinetic cleavage furrowing

Microtubules also coordinate the position of the mitotic spindle with the plane of cytokinetic cleavage (Jantsch-Plunger et al., 2000; Bringmann and Hyman, 2005; Motegi et al., 2006). We observed a significant mis-positioning of cytokinetic furrows in prefoldin-deficient embryos, and, to a lesser extent, in CCT-deficient embryos (Table 1). In most (8/10) embryos depleted of prefoldin function, more than two cytokinetic cleavage furrows ingressed. Ectopic cleavage furrows often formed on the anterior–posterior axis, bisecting the transverse central spindle. Except for the most severely affected embryos, ectopic cleavage furrows usually resolved into two furrows perpendicular to the anterior–posterior axis towards the end of cytokinesis (Fig. 5B). Cortical contractility appeared less active in *cct-1(RNAi)* embryos, such that most embryos did not have an obvious furrow and only 2/5 embryos exhibited clear mis-positioning of the cleavage furrow (Table 1, Fig. 5C).

*Meiosis*

We also found weakly penetrant meiotic defects for *pf $d$ -3* (*RNAi*) and *cct-1* (*RNAi*), whereby some embryos contained

more than two pronuclei (Table 1, data not shown, Fig. 5C). The meiotic phenotype in *pf $d$ -3* (*RNAi*) and *cct-1* (*RNAi*) embryos could result from defective meiotic spindle assembly and/or

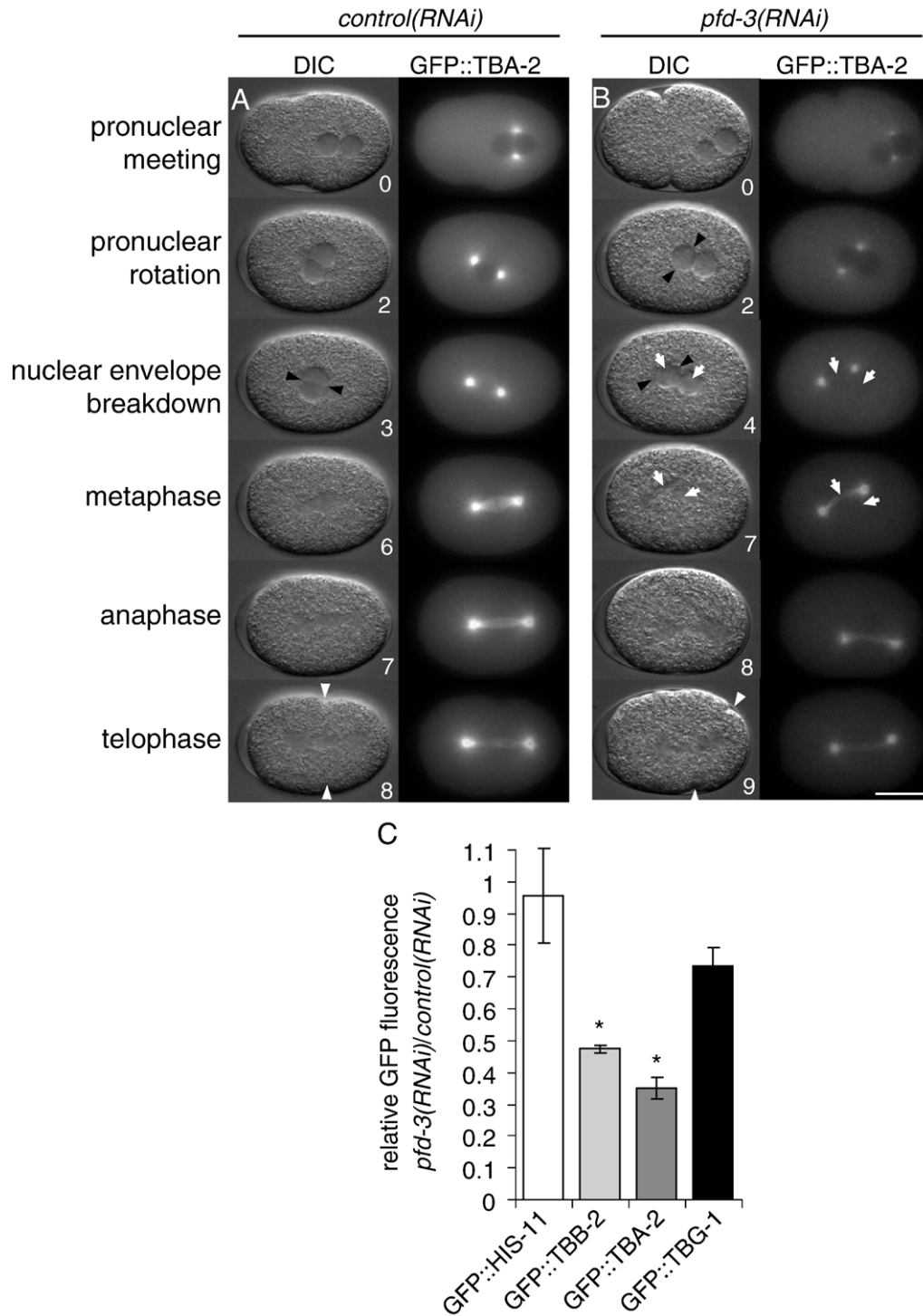


Fig. 4. Prefoldin is essential for the proper function of the microtubule cytoskeleton. Black arrowheads indicate centrosomes; white arrowheads indicate cleavage furrows. Approximate developmental time in minutes is shown. (A) Control embryo showing the behaviour of GFP::TBA-2 incorporated into microtubules during the first cell cycle. (B) Behaviour of GFP::TBA-2 in *pf $d$ -3* (*RNAi*) embryos. White arrows indicate locations of maternal and paternal chromosomes and two distinct regions of spindle microtubule outgrowth. Note asymmetrically located cleavage furrows. Scale bar=20  $\mu$ m. (C) Quantification of GFP::HIS-11, GFP::TBB-2, GFP::TBA-2 and GFP::TGB-1 fluorescence intensities in single-celled *pf $d$ -3* (*RNAi*) embryos relative to *control* (*RNAi*) embryos; GFP::TGB-1 fluorescence was quantified in the P1 cell of 2-cell stage embryos; see Materials and methods;  $n=10$  embryos each; mean $\pm$ S.E.M. shown. Stars indicate values that were significantly different from *control* (*RNAi*) in a Student's *t*-test ( $p<0.05$ ).

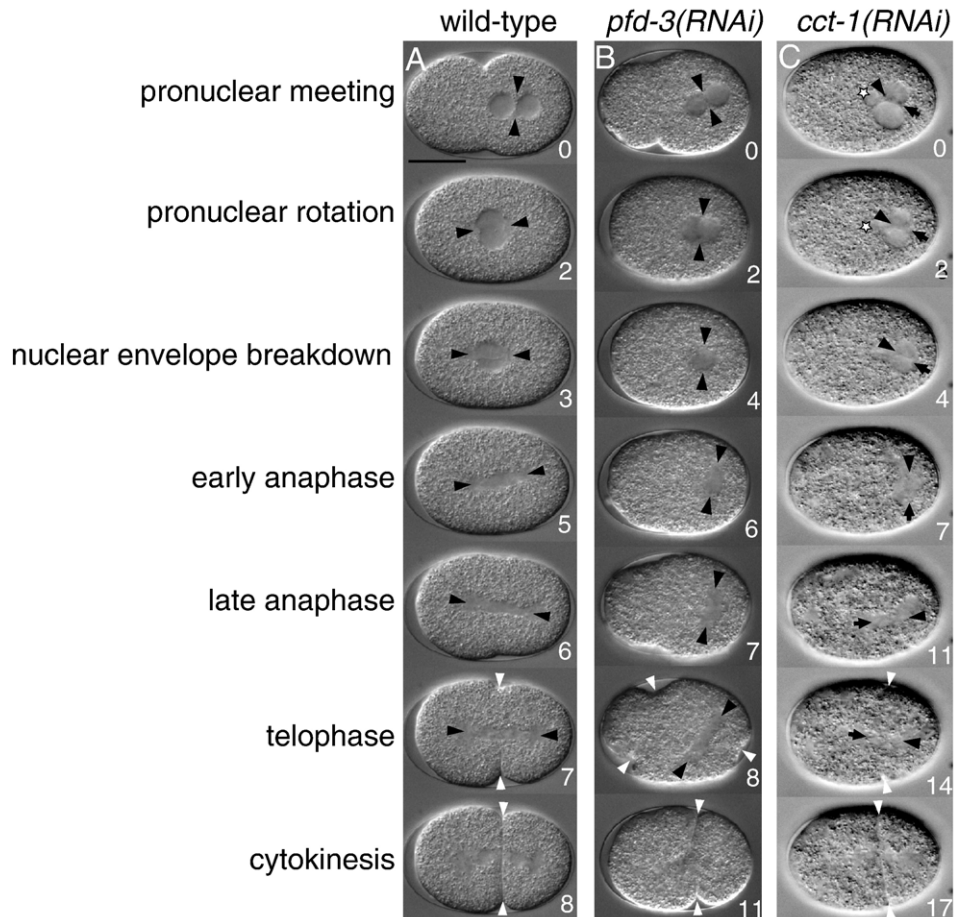


Fig. 5. Prefoldin and CCT are required for rotation of the pronuclear–centrosome complex, spindle positioning and specification of the cytokinetic cleavage furrow. Approximate time in minutes shown, black arrowheads and arrows indicate centrosomes, white arrowheads indicate cleavage furrows, and star indicates extra maternal pronucleus. (A) Scale bar=20  $\mu$ m.

problems with the extrusion of extraneous maternal DNA into polar body vesicles, a process that likely involves microfilament function (Bowerman, 2001).

#### Cytoplasmic streaming and pseudocleavage furrowing

The anterior velocity of cortical yolk granules was reduced in both *pfd-3(RNAi)* and *cct-1(RNAi)* embryos relative to control embryos (Table 1). On the other hand, both *pfd-3(RNAi)* and *cct-1(RNAi)* embryos displayed normal pseudocleavage furrowing. We expected a correlation between cytoplasmic streaming and pseudocleavage furrowing since both processes are thought to be dependent on polarized actomyosin contractile activity. However, the mechanism driving cytoplasmic streaming requires an interaction between a sperm centrosome and the cortex in a process which may also depend on astral microtubules (Hird and White, 1993; O'Connell et al., 2000; Sonnevile and Gönczy, 2004; Munro et al., 2004).

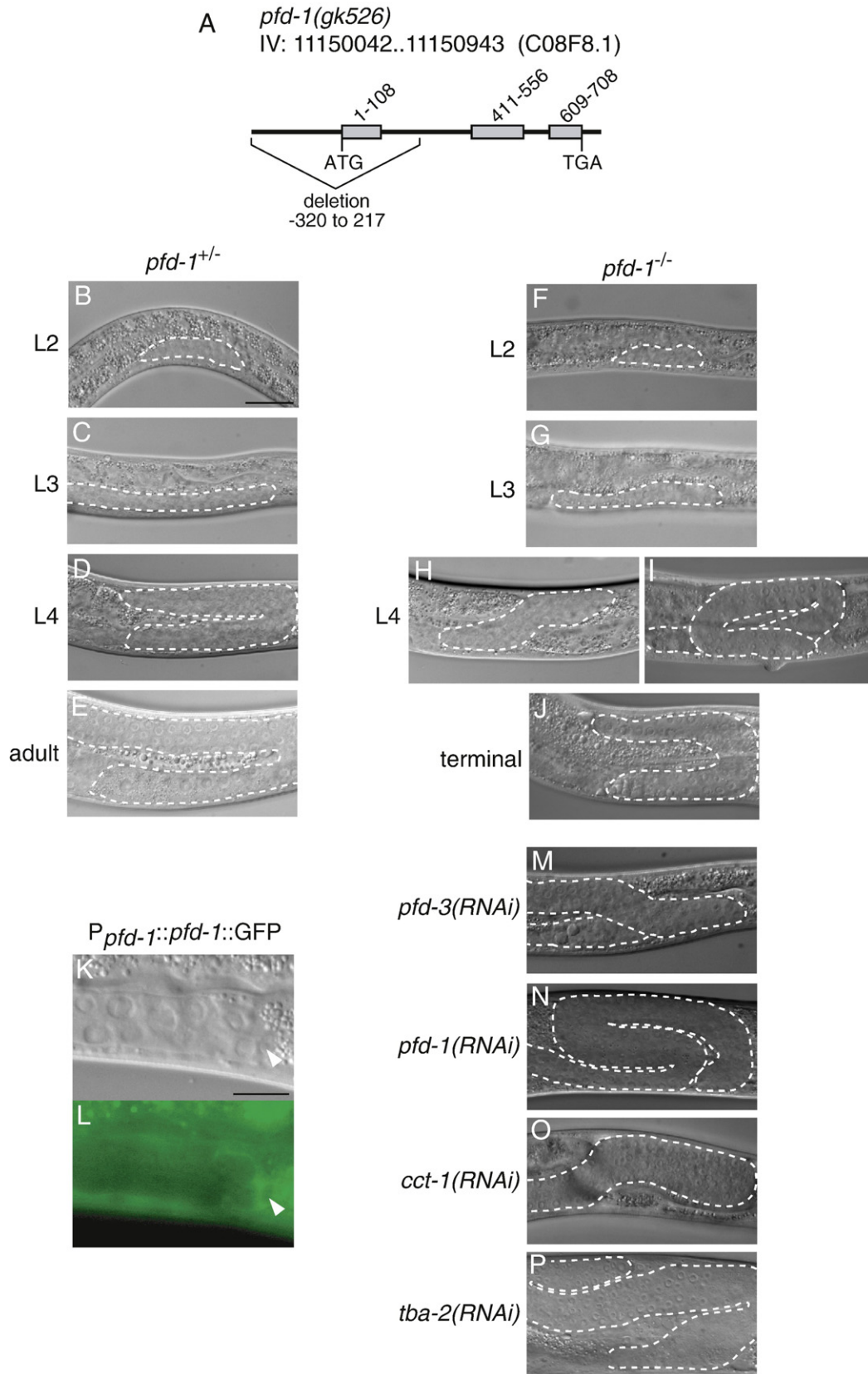
#### Chromosome segregation

We assessed the fidelity of chromosome segregation by examining the localization of GFP-tagged histone protein HIS-11, which binds to condensed chromatin. In half (5/10) of the *pfd-3(RNAi)* embryos recorded, we observed clear mis-

segregation of GFP-HIS-11-labeled chromatin during telophase of the first cell division, usually as a result of earlier defects in spindle assembly (Supplementary Fig. 4). This is similar to the situation in *S. cerevisiae*, where the loss of prefoldin function also causes a chromosome segregation defect (Vainberg et al., 1998); however, in contrast to the slow growth phenotype of yeast, the consequence of this in the *C. elegans* embryo is disruption of the developmental program and lethality.

We then sought to determine whether a deficiency in microtubule function alone could explain some, if not all, of the phenotypes observed for knockdown of prefoldin or CCT. To decrease microtubule function in the embryo, we used *tba-2(RNAi)*, which results in reduced formation of microtubules and embryonic lethality (Fraser et al., 2000; Wright and Hunter, 2003; Sonnevile and Gönczy, 2004; Phillips et al., 2004; Srayko et al., 2005; Motegi et al., 2006). Our analyses revealed that *tba-2(RNAi)* phenocopied the early embryonic defects of prefoldin or CCT knockdown, including a change in the streaming of cytoplasmic granules (Table 1).

Taken together, our studies on RNAi-treated embryos provide evidence that, although subtle effects on actin function cannot be discounted, the role of prefoldin in the early embryo is predominantly to provide an efficient folding environment for



newly translated tubulin polypeptides. Furthermore, these analyses suggest that prefoldin and CCT have largely overlapping, though seemingly not identical roles in the early embryo.

#### *Prefoldin and CCT are required for distal tip cell migration and oogenesis*

Since RNAi removes both maternal and zygotic gene products, we decided to test the requirement for zygotic *pf<sub>d</sub>-1* in *C. elegans* by observing the development of worms homozygous for a mutant allele of *pf<sub>d</sub>-1*. We obtained a strain carrying the deletion allele *pf<sub>d</sub>-1(gk526)* from the *C. elegans* Knockout Consortium that removes the first exon and 300 base-pairs of upstream sequence, and is therefore predicted to be a null allele (Fig. 6A). To our surprise, homozygous *pf<sub>d</sub>-1<sup>-/-</sup>* progeny from heterozygous *pf<sub>d</sub>-1<sup>+/-</sup>* hermaphrodites were able to complete embryogenesis and early larval development, only to cease development as L4 larvae or sterile adults.

When we examined the developing gonads of homozygous *pf<sub>d</sub>-1(gk526)* worms, we noticed striking morphological abnormalities. The characteristic C-shaped gonad morphology displayed by wild-type and heterozygous *pf<sub>d</sub>-1<sup>+/-</sup>* worms is a result of the migratory path of the somatic distal tip cell (DTC) at the leading edge of the developing gonad arm (Figs. 6B–E). DTC migration occurs in three distinct phases which are closely correlated with progression through developmental stages. The first phase involves migration away from the mid-body along the ventral body wall muscles during L2 and L3 (Figs. 6B, C). This phase appears to take place normally in *pf<sub>d</sub>-1* homozygotes (Figs. 6F, G). The second phase occurs at the end of L3 when the DTCs make a 90° turn and migrate dorsally, followed by the third phase involving another 90° turn to migrate back toward the mid-body along the dorsal body wall muscles in L4 (Fig. 6D).

We found partially penetrant DTC pathfinding defects in homozygous *pf<sub>d</sub>-1* worms (3/11 gonads had defects,  $p < 0.05$ ). In some cases, the third phase of DTC migration failed and in others, the DTCs executed supernumerary turns, both of which result in abnormal gonad morphologies (Figs. 6H, I). In light of these results, we examined the expression of *pf<sub>d</sub>-1::GFP* more closely and found that we could observe faint expression in the distal tip cell (Figs. 6K, L). The difference between the *pf<sub>d</sub>-1(RNAi)* embryonic lethal phenotype and the *pf<sub>d</sub>-1(gk526)* adult sterile phenotype suggests that the maternal contribution of *pf<sub>d</sub>-1* is significant.

To further test the requirements for prefoldin and CCT in developing larvae, we examined less severe RNAi knockdown phenotypes (Supplementary Table 1). The most prevalent post-

embryonic phenotype in *pf<sub>d</sub>(RNAi)* escape progeny was sterility (41/60 *pf<sub>d</sub>-3(RNAi)* worms; 6/59 *pf<sub>d</sub>-1(RNAi)* worms). We also observed a variety of other post-embryonic *pf<sub>d</sub>(RNAi)* phenotypes, including larval lethality, larval arrest and body morphology defects (Supplementary Table 1). Together with the observed expression patterns (Supplementary Fig. 1), these results suggest that prefoldin is required for the development of multiple tissues of the animal, especially the gonad.

When we examined the gonads of *pf<sub>d</sub>-1(RNAi)* and *pf<sub>d</sub>-3(RNAi)* sterile escape progeny we found DTC pathfinding defects similar to those found in homozygous *pf<sub>d</sub>-1(gk526)* mutant animals (3/8 *pf<sub>d</sub>-1(RNAi)* gonads and 4/9 *pf<sub>d</sub>-3(RNAi)* gonads), including a delay in dorsal turning (i.e. phase two of DTC pathfinding; Fig. 6M) and the execution of supernumerary turns (Fig. 6N). The fact that *pf<sub>d</sub>-1(RNAi)* and *pf<sub>d</sub>-3(RNAi)* progeny essentially phenocopy homozygous *pf<sub>d</sub>-1(gk526)* animals (Figs. 6H–I, M–N) confirms an important role for prefoldin in DTC migration and oogenesis.

To mimic a low level of CCT knockdown in the developing animal, we grew worms from hatching on bacteria expressing *cct-1* dsRNA (since worms injected with *cct-1* dsRNA did not produce any escape progeny with a sterile phenotype; Supplementary Table 1). Under these conditions, the majority of dsRNA-fed worms (15/24) developed into sterile adults. *cct-1(RNAi)* gonad morphology was also highly abnormal, showing either a failure in phase three of DTC migration (i.e. anterior turning) (Fig. 6O) or extra turns (data not shown). Although the prefoldin and CCT knockdown phenotypes were essentially identical, the *cct-1(RNAi)* phenotype occurred in the maternal gonad, suggesting that the requirement for CCT in the DTCs is considerably more strict. Similarly to *pf<sub>d</sub>-1(gk526)*, we did not observe a consistent defect in any specific phase of DTC migration in either *pf<sub>d</sub>(RNAi)* or *cct(RNAi)* gonads, suggesting that prefoldin and CCT are required for a common mechanism underlying all three phases of DTC migration.

Since *tba-2(RNAi)* phenocopied prefoldin or CCT depletion in the early embryo, we tested whether the DTC migration phenotypes we observed could be explained by a similar decrease in microtubule function. We grew worms from hatching on bacteria expressing *tba-2* dsRNA and the morphology of the gonads in these animals revealed evidence of defective DTC migration similar to the ‘wandering’ phenotype described above, including failure in turning (9/18 gonads) (data not shown) and extra turns (Fig. 6P). This is, to the best of our knowledge, the first time that microtubule function has been directly implicated in distal tip cell migration in *C. elegans*. As in the early embryo, the most important role for prefoldin and CCT in the distal tip cells may be to provide an efficient folding environment for nascent tubulin polypeptides.

Fig. 6. Prefoldin and CCT are required for distal tip cell migration and oogenesis. (A) Schematic diagram of predicted loss-of-function mutation in *pf<sub>d</sub>-1(gk526)* allele. Numbers represent nucleotide positions relative to the start of the ATG codon. (B–P) DIC images of posterior gonads, anterior left and ventral down. Dashed white line shows the gonad morphology and the trajectory of DTC migration. (B–J) Developmental time-course of DTC migration. Scale bar=25 μm. (B–E) *pf<sub>d</sub>-1<sup>+/-</sup>* heterozygotes; (F–J) *pf<sub>d</sub>-1<sup>-/-</sup>* homozygous worms. (K, L) *pf<sub>d</sub>-1::GFP* is expressed in the distal tip cell; white arrowhead indicates the DTC nucleus; (K) DIC; (L) GFP; scale bar=10 μm. (M–P) Low-level RNAi knockdown of prefoldin, CCT or α-tubulin causes aberrant DTC migration and failure in oogenesis. (M) Progeny of *pf<sub>d</sub>-3* dsRNA-injected worm. (N) Progeny of *pf<sub>d</sub>-1* dsRNA-injected worm. (O) Worm fed from hatching on bacteria expressing *cct-1* dsRNA. (P) Worm fed from hatching on bacteria expressing *tba-2* dsRNA.

## Discussion

### *Prefoldin function in the early embryo*

Experiments in *S. cerevisiae* and *in vitro* have shown that prefoldin binds to a specific set of nascent substrate polypeptides – including actin and tubulin – as they emerge from the ribosome and facilitates productive binding and folding inside the cavity of the CCT chaperonin (Vainberg et al., 1998; Hansen et al., 1999; Siegers et al., 1999, 2003). In this study we have analyzed the cellular and developmental requirements for prefoldin and CCT in the metazoan *C. elegans*. We demonstrate that in the absence of wild-type prefoldin function, the steady-state level of endogenous  $\alpha$ -tubulin in the embryo was decreased by 95% (Figs. 2A, B), consistent with a reduced efficiency of  $\alpha$ -tubulin folding and an increase in the production of non-native  $\alpha$ -tubulin that is subsequently removed from the cell by proteolysis. This was associated with a decrease in the microtubule growth rate and an overall reduction in the number of microtubules—particularly long astral microtubules (Figs. 2 and 4, Movies S1, S2). The cell division phenotypes observed in prefoldin-deficient embryonic cells, including the failure in pronuclear–centrosome rotation, aberrant mitotic spindle positioning and chromosome segregation (Table 1, Fig. 5), can be explained by a reduction in the number of these long microtubules interacting with the cortex or the kinetochores (Hyman and White, 1987; Wright and Hunter, 2003; Phillips et al., 2004; Motegi et al., 2006).

Our results also show that the concentration of actin was reduced by 30% in prefoldin-depleted embryos (Fig. 2B) and that there was little or no effect on the microfilament-dependent functions tested (Table 1, Fig. 3). This was surprising given the extensive literature on the role of prefoldin in actin biogenesis (Vainberg et al., 1998; Geissler et al., 1998; Siegers et al., 1999; Stirling et al., 2006). These results suggest that, compared to tubulin, actin has a slow turnover in the embryo and few polypeptides are being translated that require folding. The rapid succession of multiple rounds of mitosis in the early *C. elegans* embryo may require a higher rate of tubulin synthesis and folding than actin biogenesis. In fact, it is likely that the relative rates of synthesis of actin and tubulin are tightly regulated according to the specific needs of the cell. In mouse mammary cells, the levels of tubulin and CCT proteins varied with growth rate while actin protein levels remained relatively constant (Yokota et al., 1999). Thus, the load of these two prefoldin client proteins likely varies with developmental time and across cell types. Moreover, since both actin and tubulin require CCT for reaching the native state, they likely compete for prefoldin binding and access to the limited folding space within the CCT cavity. The coordinated action of prefoldin and other CCT cofactors, such as the phospho-ubiquitin-like proteins (Stirling et al., 2006, 2007), may account for a complex and dynamic regulation of CCT-mediated cytoskeletal protein folding.

In light of the limited evidence supporting  $\gamma$ -tubulin as a prefoldin substrate (Geissler et al., 1998), the fact that we could not detect a significant decrease in the steady-state  $\gamma$ -tubulin concentration (Fig. 2B) or any severe centrosome malfunction

in *pf $\delta$ -3(RNAi)* embryonic cells (Supplementary Fig. 3), suggests that  $\gamma$ -tubulin may not be a substrate of prefoldin, and that the reported interaction between  $\gamma$ -tubulin and prefoldin (Geissler et al., 1998) is indicative of some function other than CCT-mediated folding (Melki et al., 1993). Alternatively, our  $\gamma$ -tubulin results may reflect a slow turnover rate such that newly translated  $\gamma$ -tubulin does not represent a significant substrate load for prefoldin in embryonic cells of *C. elegans*.

In *S. cerevisiae*, slow accumulation of native actin and tubulin through prefoldin-independent folding pathways is sufficient for viability, although some of the cells are not viable and contribute to the slow growth rate of prefoldin deletion strains (Siegers et al., 1999). The development of a multicellular organism such as *C. elegans* depends on the coordinated proliferation, migration and differentiation of cells within the embryo. Microtubule defects (and associated downstream effects), similar to those we observe in the early cell divisions of *pf $\delta$ -3(RNAi)* embryos, are sufficient to cause embryonic lethality (Fraser et al., 2000; Wright and Hunter, 2003; Phillips et al., 2004). Therefore, although it is possible that actin or other substrates contribute to the essential function of prefoldin, we suggest that the reason prefoldin is essential for viability in *C. elegans* and not in *S. cerevisiae* is due to a strict dependence on efficient tubulin biogenesis during metazoan development.

### *CCT function in C. elegans*

As predicted from their functional cooperation *in vitro*, prefoldin and CCT knockdown caused similar phenotypes (Table 1, Figs. 5 and 6). However, RNAi-knockdown of CCT caused more severe phenotypes both in the embryo and developing gonad, suggesting a more stringent requirement for CCT than for prefoldin. This is consistent with the observations that actin and tubulin are absolutely dependent on CCT to reach the native state, while prefoldin simply increases the efficiency of the CCT-mediated folding reaction (Gao et al., 1992; Yaffe et al., 1992; Siegers et al., 1999) and that CCT folds additional essential proteins such as Cdc20 and Cdc55, independently of prefoldin (Camasses et al., 2003; Siegers et al., 2003). Finally, the progression of cell cycle events were delayed in *cct-1(RNAi)* embryos (Fig. 6C), consistent with the notion that CCT is ‘hard-wired’ into the regulation of the cell cycle (Grantham et al., 2006).

### *Prefoldin and CCT function in post-embryonic development*

Our analyses of RNAi-knockdown and mutant phenotypes demonstrate a role for prefoldin and CCT in distal tip cell migration in the developing gonad (Fig. 6). Our results suggest that the DTC pathfinding defects in prefoldin- and CCT-deficient worms are due to the functions of these chaperones in the DTCs (i.e. DTC-intrinsic factors) rather than problems due to cell proliferation or disruption of the migratory substrate. First, transgenic PFD-1::GFP expression was observed in the DTCs (Figs. 6K, L). Second, DTCs localize correctly to the leading edge of migrating gonads in *pf $\delta$ -1(gk526)*, *pf $\delta$ (RNAi)*

and *cct-1(RNAi)* worms (data not shown). Finally, we observed no obvious defects in the locomotory behaviour of *pf1d-1(gk526)*, *pf1d(RNAi)*, *cct-1(RNAi)* or *tba-2(RNAi)* worms that were DTC pathfinding-defective, suggesting that the body wall muscles, which serve as the migratory substrate, are intact.

Studies from yeast and mammalian cells have shown that conserved microtubule plus-end binding proteins such as EB1/Bim1 and CLIP-170/Bik1 mediate cortical capture of microtubules during both cell division and cell migration (Gundersen et al., 2004). Our results show that tubulin knockdown phenocopies either prefoldin or CCT knockdown in both the embryo and in the DTCs (Table 1, Fig. 6). While our results do not distinguish between the relative contributions of actin and tubulin deficiency in the DTC's, we propose that defective cell migration of the DTCs and the cell division phenotypes in the early embryo are mainly the result of the same underlying deficiency in chaperone-mediated tubulin folding. We speculate that a low level of prefoldin or CCT depletion in the developing worm causes a small reduction in tubulin levels and microtubule dynamics in the DTCs, which in turn results in poorly regulated cortex–microtubule interactions and a ‘wandering’ cell migration phenotype.

In conclusion, our studies suggest that efficient prefoldin- and CCT-mediated cytoskeletal protein folding – and tubulin folding in particular – is required for embryonic cell division and for certain aspects of gonadogenesis including distal tip cell migration. In light of our results, we speculate that a high rate of degradation and *de novo* synthesis of tubulin, and therefore a strict dependence on efficient chaperone-mediated folding, may be a general requirement for metazoan cells with a dynamic microtubule cytoskeleton such as dividing and migrating cells.

## Acknowledgments

We thank M. Wakayama, R. Schnabel, D. Moerman, N. Hawkins, A. Ma, K. Hingwing, G. Alfaro, P. Stirling and members of the Leroux lab for technical assistance and helpful discussions. We thank Dr. David Baillie, the *Caenorhabditis* Genetics Center, which is funded by the National Institutes of Health, and the *C. elegans* Knockout Consortium for providing strains. This work was funded by the Canadian Institutes of Health Research (CIHR; grant BMA121093). M. R. L. is supported by scholar awards from CIHR and the Michael Smith Foundation for Health Research (MSFHR).

## Appendix A. Supplementary data

Supplementary data associated with this article can be found, in the online version, at doi:10.1016/j.ydbio.2007.10.022.

## References

Ansley, et al., 2003. Basal body dysfunction is a likely cause of pleiotropic Bardet–Biedl syndrome. *Nature* 425, 628–633.  
 Bartolini, et al., 2005. Identification of a novel tubulin-stabilizing protein related to the chaperone cofactor E. *J. Cell. Sci.* 118, 1197–1207.  
 Bowerman, B., 2001. Cytokinesis in the *C. elegans* embryo: regulating

contractile forces and a late role for the central spindle. *Cell Struct. Funct.* 26, 603–607.  
 Brenner, S., 1974. The genetics of *Caenorhabditis elegans*. *Genetics* 77, 71–94.  
 Bringmann, H., Hyman, A.A., 2005. A cytokinesis furrow is positioned by two consecutive signals. *Nature* 436, 731–734.  
 Camasses, et al., 2003. The CCT chaperonin promotes activation of the anaphase-promoting complex through the generation of functional Cdc20. *Mol. Cell* 12, 87–100.  
 Chen, et al., 2005. WormBase: a comprehensive data resource for *Caenorhabditis* biology and genomics. *Nucleic Acids Res.* 33, D383–D389.  
 Dammermann, et al., 2004. Centriole assembly requires both centriolar and pericentriolar matrix proteins. *Dev. Cell* 7, 815–829.  
 Ellis, et al., 2003. Maternally expressed and partially redundant  $\beta$ -tubulins in *Caenorhabditis elegans* are autoregulated. *J. Cell. Sci.* 117, 457–464.  
 Fire, et al., 1998. Potent and specific genetic interference by double-stranded RNA in *Caenorhabditis elegans*. *Nature* 391, 806–811.  
 Fraser, et al., 2000. Functional genomic analysis of *C. elegans* chromosome I by systematic RNA interference. *Nature* 408, 325–330.  
 Gao, et al., 1992. A cytoplasmic chaperonin that catalyzes  $\beta$ -actin folding. *Cell* 69, 1043–1050.  
 Gay, 1989. Autoregulatory control of  $\beta$ -tubulin mRNA stability in linked to translation elongation. *Proc. Natl. Acad. Sci. U. S. A.* 86, 5763–5767.  
 Geissler, et al., 1998. A novel protein complex promoting formation of functional  $\alpha$ - and  $\gamma$ -tubulin. *EMBO J.* 17, 952–966.  
 Grantham, et al., 2006. Substantial CCT activity is required for cell cycle progression and cytoskeletal organization in mammalian cells. *Exp. Cell Res.* 312, 2309–2324.  
 Gönczy, et al., 2000. Functional genomic analysis of cell division in *C. elegans* using RNAi of genes on chromosome III. *Nature* 408, 331–336.  
 Gstaiger, et al., 2003. Control of nutrient-sensitive transcription programs by the unconventional prefoldin URI. *Science* 302, 1208–1212.  
 Gundersen, et al., 2004. Cortical control of microtubule stability and polarization. *Curr. Opin. Cell Biol.* 16, 106–112.  
 Guo, S., Kempfues, K.J., 1996. A non-muscle myosin required for embryonic polarity in *Caenorhabditis elegans*. *Nature* 382, 455–458.  
 Hannak, et al., 2002. The kinetically dominant assembly pathway for centrosomal asters in *Caenorhabditis elegans* is gamma-tubulin dependent. *J. Cell Biol.* 157, 591–602.  
 Hansen, et al., 1999. Prefoldin-nascent chain complexes in the folding of cytoskeletal proteins. *J. Cell Biol.* 145, 265–277.  
 Hartl, F.U., Hayer-Hartl, M., 2002. Molecular chaperones in the cytosol: from nascent chain to folded protein. *Science* 295, 1852–1859.  
 Her, et al., 2003. Human MutS homolog MSH4 physically interacts with von Hippel-Lindau tumor suppressor-binding protein 1. *Cancer Res.* 63, 865–872.  
 Hill, et al., 2000. Genomic analysis of gene expression in *C. elegans*. *Science* 290, 809–812.  
 Hird, S.N., White, J.G., 1993. Cortical and cytoplasmic flow polarity in early embryonic cells of *Caenorhabditis elegans*. *J. Cell Biol.* 121, 1343–1355.  
 Hyman, A.A., White, J.G., 1987. Determination of cell division axes in the early embryogenesis of *Caenorhabditis elegans*. *J. Cell Biol.* 105, 2123–2135.  
 Jantsch-Plunger, 2000. CYK-4: a Rho family gtpase activating protein (GAP) required for central spindle formation and cytokinesis. *J. Cell Biol.* 149, 1391–1404.  
 Kamath, et al., 2003. Systematic functional analysis of the *Caenorhabditis elegans* genome using RNAi. *Nature* 421, 231–237.  
 Kelly, et al., 1997. Distinct requirements for somatic and germline expression of a generally expressed *Caenorhabditis elegans* gene. *Genetics* 146, 227–238.  
 Kirkham, et al., 2003. SAS-4 is a centriolar protein that controls centrosome size. *Cell* 112, 575–587.  
 Labbe, et al., 2003. PAR proteins regulate microtubule dynamics at the cell cortex in *C. elegans*. *Curr. Biol.* 13, 707–714.  
 Lacefield, S., Solomon, F., 2003. A novel step in  $\beta$ -tubulin folding is important for heterodimer formation in *Saccharomyces cerevisiae*. *Genetics* 165, 531–541.  
 Lacefield, et al., 2006. Consequences of defective tubulin folding on

- heterodimer levels, mitosis and spindle morphology in *Saccharomyces cerevisiae*. *Genetics* 173, 635–646.
- Le Bot, et al., 2003. TAC-1, a regulator of microtubule length in the *C. elegans* embryo. *Curr. Biol.* 13, 1499–1505.
- Leroux, M.R., Candido, P.M., 1997. Subunit characterization of the *Caenorhabditis elegans* chaperonin containing TCP-1 and expression pattern of the gene encoding CCT-1. *Biochem. Biophys. Res. Commun.* 241, 687–692.
- Leroux, M.R., Hartl, F.U., 2000. Protein folding: versatility of the cytosolic chaperonin TRiC/CCT. *Curr. Biol.* 10, R260–R264.
- Leroux, et al., 1999. MtGimC, a novel archaeal chaperone related to the eukaryotic chaperonin cofactor GimC/prefoldin. *EMBO J.* 18, 6730–6743.
- Liu, et al., 2005. CCT chaperonin complex is required for the biogenesis of functional Plk1. *Mol. Cell. Biol.* 25, 4993–5010.
- Llorca, et al., 2000. Eukaryotic chaperonin CCT stabilizes actin and tubulin folding intermediates in open quasi-native conformations. *EMBO J.* 19, 5971–5979.
- Lopez-Fanarraga, et al., 2001. Review: postchaperonin tubulin folding cofactors and their role in microtubule dynamics. *J. Struct. Biol.* 135, 219–229.
- Lundin, et al., 2004. Molecular clamp mechanism of substrate binding by hydrophobic coiled coil resides of the archaeal chaperone prefoldin. *PNAS* 101, 4367–4372.
- Maeda, et al., 2001. Large-scale analysis of gene function in *Caenorhabditis elegans* by high-throughput RNAi. *Curr. Biol.* 11, 171–176.
- Martin-Benito, et al., 2002. Structure of eukaryotic prefoldin and of its complexes with unfolded actin and the cytosolic chaperonin CCT. *EMBO J.* 21, 6377–6386.
- Martin-Benito, et al., 2007. Divergent substrate-binding mechanisms reveal an evolutionary specialization of eukaryotic prefoldin compared to its archaeal counterpart. *Structure* 15, 101–110.
- McKay, et al., 2003. Gene expression profiling of cells, tissues, and developmental stages of the nematode *C. elegans*. *Cold Spring Harbor Symp. Quant. Biol.* 68, 159–169.
- Melki, et al., 1993. Chaperonin-mediated folding of vertebrate actin-related protein and  $\gamma$ -tubulin. *J. Cell Biol.* 122, 1301–1310.
- McLaughlin, et al., 2002. Regulatory interaction of phospho-ducin-like protein with the cytosolic chaperonin complex. *PNAS* 99, 7962–7967.
- Mitchison, T., Kirschner, M., 1984. Dynamic instability of microtubule growth. *Nature* 312, 237–242.
- Mori, et al., 1998. MM-1, a novel c-Myc-associating protein that represses transcriptional activity of c-Myc. *J. Biol. Chem.* 273, 29794–29800.
- Motegi, et al., 2006. Two phases of astral microtubule activity during cytokinesis in *C. elegans* embryos. *Dev. Cell* 10, 509–520.
- Munro, et al., 2004. Cortical flows powered by asymmetrical contraction transport PAR proteins to establish and maintain anterior–posterior polarity in the early *C. elegans* embryo. *Dev. Cell* 7, 413–424.
- O’Connell, et al., 2000. The *spd-2* gene is required for polarization of the anteroposterior axis and formation of the sperm asters in the *Caenorhabditis elegans* zygote. *Dev. Biol.* 222, 55–70.
- Ogawa, et al., 2004. An evolutionary conserved gene required for proper microtubule architecture in *Caenorhabditis elegans*. *Genes Cells* 9, 83–93.
- Okochi, et al., 2004. Kinetics and binding sites for interaction of the prefoldin with a group II chaperonin. *J. Biol. Chem.* 279, 31788–31795.
- Phillips, et al., 2004. Roles for two partially redundant  $\alpha$ -tubulins during mitosis in early *Caenorhabditis elegans* embryos. *Cell Motil. Cytoskelet.* 58, 112–126.
- Quintin, et al., 2003. The *mbk-2* kinase is required for inactivation of MEI-1/katanin in the one-cell *Caenorhabditis elegans* embryo. *EMBO Rep.* 4, 1175–1181.
- Savage, et al., 1994. Mutations in the *Caenorhabditis elegans* b-tubulin gene *mec-7*: effects on microtubule assembly and stability and on tubulin autoregulation. *J. Cell. Sci.* 107, 2165–2175.
- Siegers, et al., 1999. Compartmentation of protein folding in vivo: sequestration of non-native polypeptide by the chaperonin–GimC system. *EMBO J.* 18, 75–84.
- Siegers, et al., 2003. TRiC/CCT cooperates with different upstream chaperones in the folding of distinct protein classes. *EMBO J.* 22, 5230–5240.
- Siebert, et al., 2000. Structure of the molecular chaperone prefoldin: unique interaction of multiple coiled coil tentacles with unfolded proteins. *Cell* 103, 621–632.
- Simmer, et al., 2003. Genome-wide RNAi of *C. elegans* using the hypersensitive *rrf-3* strain reveals novel gene functions. *PLoS Biol.* 1, 77–84.
- Simons, et al., 2004. Selective contribution of eukaryotic prefoldin subunits to actin and tubulin binding. *J. Biol. Chem.* 279, 4196–4203.
- Sonneville, R., Gönczy, P., 2004. *zyg-9* and *cul-2* regulate progression through meiosis II and polarity establishment in *C. elegans*. *Development* 131, 3527–3543.
- Sönnichsen, et al., 2005. Full-genome RNAi profiling of early embryogenesis in *Caenorhabditis elegans*. *Nature* 434, 462–469.
- Spieß, et al., 2004. Mechanism of the eukaryotic chaperonin: protein folding in the chamber of secrets. *TRENDS Cell Biol.* 14, 598–604.
- Srayko, et al., 2005. Identification and characterization of factors required for microtubule growth and nucleation in the early *C. elegans* embryo. *Dev. Cell* 9, 223–236.
- Sternlicht, et al., 1993. The t-complex polypeptide complex is a chaperonin for tubulin and actin in vivo. *Proc. Natl. Acad. Sci. U. S. A.* 90, 9422–9426.
- Stirling, et al., 2006. PhLP modulates CCT-mediated actin and tubulin folding via ternary complexes with substrates. *J. Biol. Chem.* 281, 7012–7021.
- Stirling, et al., 2007. Functional interaction between phospho-ducin-like protein 2 and cytosolic chaperonin is essential for cytoskeletal protein function and cell cycle progression. *Mol. Biol. Cell* 18, 2336–2345.
- Strome, S., Wood, W.B., 1983. Generation of asymmetry and segregation of germ-line granules in early *C. elegans* embryos. *Cell* 35, 15–25.
- Thulasiraman, et al., 1999. In vivo translated polypeptides are sequestered in a protected folding environment. *EMBO J.* 18, 85–95.
- Timmons, L., Fire, A., 1998. Specific interference by ingested dsRNA. *Nature* 395, 854.
- Tsuchiya, et al., 1996. Identification of a novel protein (VBP-1) binding to the von Hippel-Lindau (VHL) tumor suppressor gene product. *Cancer Res.* 56, 2881–2885.
- Vainberg, et al., 1998. Prefoldin, a chaperone that delivers unfolded proteins to cytosolic chaperonin. *Cell* 93, 863–873.
- Walker, et al., 1988. Dynamic instability of individual microtubules analyzed by light microscopy: rate constants and transition frequencies. *J. Cell Biol.* 107, 1437–1448.
- Willison, K.R., 1999. Composition and function of the eukaryotic cytosolic chaperonin-containing TCP-1. In: Bukau, B. (Ed.), *Molecular Chaperones: Frontiers in Molecular Biology*. Oxford University Press, Oxford.
- Wright, A.J., Hunter, C.P., 2003. Mutations in a  $\beta$ -tubulin disrupt spindle orientation and microtubule dynamics in the early *Caenorhabditis elegans* embryo. *Mol. Biol. Cell* 14, 4512–4525.
- Yaffe, et al., 1992. TCP1 complex is a molecular chaperone in tubulin biogenesis. *Nature* 358, 245–248.
- Yokota, et al., 1999. Cytosolic chaperonin is up-regulated during cell growth. *J. Biol. Chem.* 274, 37070–37078.
- Zako, et al., 2005. Facilitated release of substrate protein from prefoldin by chaperonin. *FEBS Lett.* 579, 3718–3724.
- Zipperlen, et al., 2001. Roles for 147 embryonic lethal genes on *C. elegans* chromosome I identified by RNA interference and video microscopy. *EMBO J.* 20, 3984–3992.